Tracer Advection II: Advanced Numerical Methods for Transport Problems

Ram Nair

Computational and Information Systems Laboratory (CISL)
National Center for Atmospheric Research
Boulder, CO, USA.

[The 2012 Dynamical Core Model Intercomparison Project: DCMIP Workshop, August 8th]

NCAR

Atmospheric Numerical Modeling : [Desirable Properties]

Numerical algorithms for the next generation atmospheric models should be based on the following criteria:

- Inherent local and global conservation
- High-order accuracy
- Computational efficiency
- Geometric flexibility (complex domain boundaries, AMR capability)
- Non-oscillatory advection (monotonic or positivity preservation)
- High parallel efficiency (local method, petascale capability aiming $O(100K)$ processors)

- Examples of numerical methods which can address the above requirements:- Continuous Galerkin or Spectral Element (SE) method, Multimoment Finite-Volume (FV) Method and Discontinuous Galerkin (DG) Method etc..
- The DG method (DGM) is a hybrid approach which combines nice features of SE and FV methods

Part-I

- How to solve the basic building block of a complex model – the advection problem – with DGM?

Flux-Form Atmospheric Equations (Conservation Laws)

- A large class of atmospheric equations of motion for compressible and incompressible flows can be written in flux (conservation) form.
- Conservation laws are systems of nonlinear partial differential equations (PDEs) in flux form and can be written:

$$\frac{\partial}{\partial t} U(\mathbf{x}, t) + \sum_{j=1}^{3} \frac{\partial}{\partial x_j} F_j(U, \mathbf{x}, t) = S(U),$$

where

  - $\mathbf{x}$ is the 3D space coordinate and time $t > 0$. $U(\mathbf{x}, t)$ is the state vector represents mass, momentum and energy etc.
  - $F_j(U)$ are given flux vectors and include diffusive and convective effects
  - $S(U)$ is the source term

- Linear transport problem is a simple example of conservation law:

$$\frac{\partial \rho}{\partial t} + \nabla \cdot (\rho \mathbf{V}) = 0, \quad \text{or } \rho_t + \mathrm{div}(\rho \mathbf{V}) = 0$$

Discontinuous Galerkin Method (DGM) in 1D

- 1D scalar conversation law:

$$
\begin{aligned}
\frac{\partial U}{\partial t} + \frac{\partial F(U)}{\partial x} &= 0 \quad \text{in} \quad \Omega \times (0, T), \\
U_0(x) &= U(x, t = 0), \quad \forall x \in \Omega
\end{aligned}
$$

- E.g., $F(U) = c\,U$ (Linear advection), $F(U) = U^2/2$ (Burgers' Equation)

- The domain Ω (periodic) is partitioned into N_x non-overlapping elements (intervals) $I_j = [x_{j-1/2}, x_{j+1/2}]$, $j = 1, \ldots, N_x$, and $\Delta x_j = (x_{j+1/2} - x_{j-1/2})$

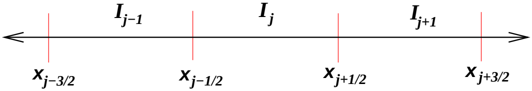

DGM-1D: Weak Formulation

A weak formulation of the problem for the approximate solution U_h is obtained by multiplying the PDE by a *test* function $\varphi_h(x)$ and integrating over an element I_j:

$$\int_{I_j} \left[\frac{\partial U_h}{\partial t} + \frac{\partial F(U_h)}{\partial x} \right] \varphi_h(x) dx = 0, \quad U_h, \varphi_h \in \mathcal{V}_h$$

Integrating the second term by parts $\Longrightarrow$

$$\int_{I_j} \frac{\partial U_h(x,t)}{\partial t} \varphi_h(x) dx - \int_{I_j} F(U_h(x,t)) \frac{\partial \varphi_h}{\partial x} dx +$$
$$F(U_h(x_{j+1/2},t))\, \varphi_h(x^-_{j+1/2}) - F(U_h(x_{j-1/2},t))\, \varphi_h(x^+_{j-1/2}) = 0,$$

where $\varphi(x^-)$ and $\varphi(x^+)$ denote "left" and "right" limits.

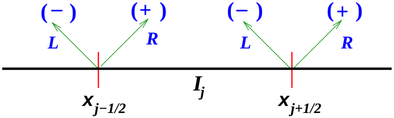

DGM-1D: Flux term ("Gluing" the discontinuous element edges)

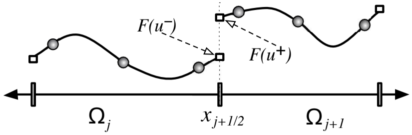

- Flux function $F(U_h)$ is discontinuous at the interfaces $x_{j\pm1/2}$
- $F(U_h)$ is replaced by a numerical flux function $\hat{F}(U_h)$, dependent on the left and right limits of the discontinuous function U. At the interface $x_{j+1/2}$,

$$\hat{F}(U_h)_{j+1/2}(t) = \hat{F}(U_h(x^-_{j+1/2}, t), U_h(x^+_{j+1/2}, t))$$

- Typical flux formulae (Approx. Reimann Solvers): Gudunov, Lax-Friedrichs, Roe, HLLC, etc.
- Lax-Friedrichs nurmerical flux formula:-

$$\hat{F}(U_h) = \frac{1}{2}\left[(F(U_h^-) + F(U_h^+)) - \alpha(U_h^+ - U_h^-)\right].$$

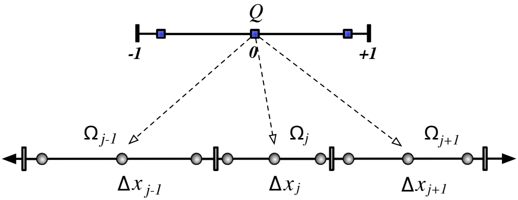

- Map every element Ω_j onto the reference element $[-1,+1]$ by introducing a local coordinate $\xi \in [-1,+1]$ s.t.,

$$\xi = \frac{2\,(x - x_j)}{\Delta x_j},\ x_j = (x_{j-1/2} + x_{j+1/2})/2 \ \Rightarrow \quad \frac{\partial}{\partial x} = \frac{2}{\Delta x_j}\frac{\partial}{\partial \xi}.$$

- Use a high-order Gaussian quadrature such as the Gauss-Legendre (GL) or Gauss-Lobatto-Legendre (GLL) quadrature rule. The GLL qudrature is 'exact' for polynomials of degree up to $2N-1$.

$$\int_{-1}^{1} f(\xi)d\xi \approx \sum_{n=0}^{N} w_n f(\xi_n); \quad \text{for GLL}, \quad \xi_n \Leftarrow (1-\xi^2)P'_\ell(\xi) = 0$$

DGM-1D: Representation of Test function & Approximate Solution

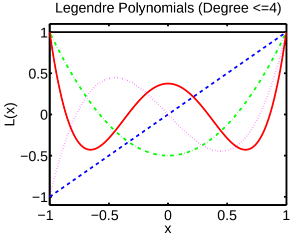

- The model basis set for the $\mathcal{P}^k$ DG method consists of Legendre polynomials, $\mathcal{B} = \{P_\ell(\xi), \ell = 0, 1, \ldots, k\}$.
- Test function $\varphi_h(x)$ and approximate solution $U_h(x)$ belong to $\mathcal{B}$

$$U_h(\xi, t) = \sum_{\ell=0}^{k} U_h^\ell(t)\, P_\ell(\xi) \quad \text{for} \quad -1 \le \xi \le 1, \quad \text{where}$$

$$U_h^\ell(t) = \frac{2\ell+1}{2} \int_{-1}^{1} U_h(\xi, t)\, P_\ell(\xi)\, d\xi \quad \ell = 0, 1, \ldots, k.$$

$$\int_{-1}^{1} P_m(x) P_n(x) dx = \frac{2}{2m+1} \delta_{m,n} \quad \Leftarrow \text{Orthogonality}$$

- $U_h^\ell(t)$ is the degrees of freedom (*dof*) evolves w.r.t time.

DGM-1D: Modal Basis Set for a "$\mathcal{P}^2$" Method

- For the $\mathcal{P}^2$ method, $\mathcal{B} = \{P_0, P_1, P_2\} = \{1, \xi, (3\xi^2 - 1)/2\}$.
- Approximate solution:

$$U_h(\xi,t) = U_h^0(t) + U_h^1(t)\,\xi + U_h^2(t)\,[3\xi^2 - 1]$$

- The *degrees of freedom* to evolve in t are:

$$\begin{aligned}
U_h^0(t) &= \frac{1}{2}\int_{-1}^{1} U_h(\xi,t)d\xi \quad \Leftarrow \text{Average} \\
U_h^1(t) &= \frac{3}{2}\int_{-1}^{1} U_h(\xi,t)\,\xi d\xi \\
U_h^2(t) &= \frac{5}{2}\int_{-1}^{1} U_h(\xi,t)\,[3\xi^2 - 1]\,d\xi
\end{aligned}$$

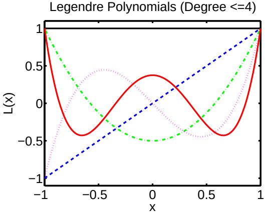

DGM-1D: Orthogonal Basis Set (Modal Vs Nodal)

Modal basis functions | Nodal basis functions

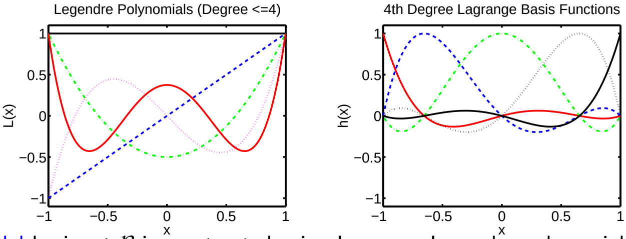

- The nodal basis set $\mathcal{B}$ is constructed using Lagrange-Legendre polynomials $h_i(\xi)$ with roots at Gauss-Lobatto quadrature points (physical space).

$$
\begin{aligned}
U_j(\xi) &= \sum_{j=0}^{k} U_j\, h_j(\xi) \quad \text{for} \quad -1 \le \xi \le 1, \\
h_j(\xi) &= \frac{(\xi^2-1)\, P_k'(\xi)}{k(k+1)\, P_k(\xi_j)\,(\xi-\xi_j)}, \quad \int_{-1}^{1} h_i(\xi) h_j(\xi) = w_i \delta_{ij}.
\end{aligned}
$$

- Nodal version was shown to be more computationally efficient than the Modal version (see, *Levy, Nair & Tufo, Comput. & Geos. 2007*)
- Modal version is more "friendly" with monotic limiting

DG-1D: Semi-Discretized Form

- Finally, the weak formulation leads the PDE to the time dependent ODE

$$\int_{I_j} \left[\frac{\partial U_h}{\partial t} + \frac{\partial F(U_h)}{\partial x} \right] \varphi_h(x) dx = 0 \Rightarrow \quad \frac{d}{dt} U_h^{\ell}(t) = \mathcal{L}(U_h) \quad \text{in}\,(0, T) \times \Omega$$

Example: For the $\mathcal{P}^1$ case on an element I_j, we need to solve:

$$\begin{aligned} \frac{d}{dt} U_h^0(t) &= \frac{-1}{\Delta x_j} \left[F(\xi = 1, t) - F(\xi = -1, t) \right] \\ \frac{d}{dt} U_h^1(t) &= \frac{-3}{\Delta x_j} \left(\left[F(\xi = 1, t) + F(\xi = -1, t) \right] - \int_{-1}^{1} U_h(\xi, t)\, d\xi \right) \end{aligned}$$

Solve the ODEs for the modes at new time level $U_h^{\ell}(t + \Delta t)$ For the $\mathcal{P}^1$ case,

$$U_h(\xi, t + \Delta t) = U_h^0(t + \Delta t) + U_h^1(\xi, t + \Delta t)\, \xi$$

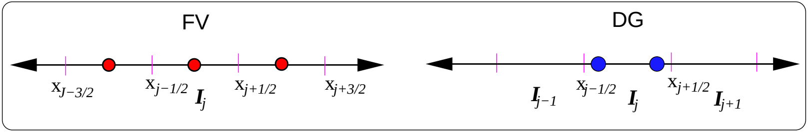

Time Integration

- For the ODE of the form,

$$\frac{d}{dt}U(t) = \mathcal{L}(U) \quad \text{in}\,(0, T) \times \Omega$$

- Strong Stability Preserving third-order Runge-Kutta (SSP-RK) scheme (*Gottlieb et al., SIAM Review, 2001*)

$$\begin{aligned}
U^{(1)} &= U^n + \Delta t \mathcal{L}(U^n) \\
U^{(2)} &= \frac{3}{4}U^n + \frac{1}{4}U^{(1)} + \frac{1}{4}\Delta t \mathcal{L}(U^{(1)}) \\
U^{n+1} &= \frac{1}{3}U^n + \frac{2}{3}U^{(2)} + \frac{2}{3}\Delta t \mathcal{L}(U^{(2)}).
\end{aligned}$$

- CFL for the DG scheme is estimated to be $1/(2k+1)$, where k is the degree of the polynomial (*Cockburn and Shu, 1989*).
- Remedy: Use low-order polynomials ($k \leq 3$) or efficient semi-implicit / implicit time integrators or high-order multi-stage R-K method.

DGM-1D: Results (Simple Linear Advection Test)

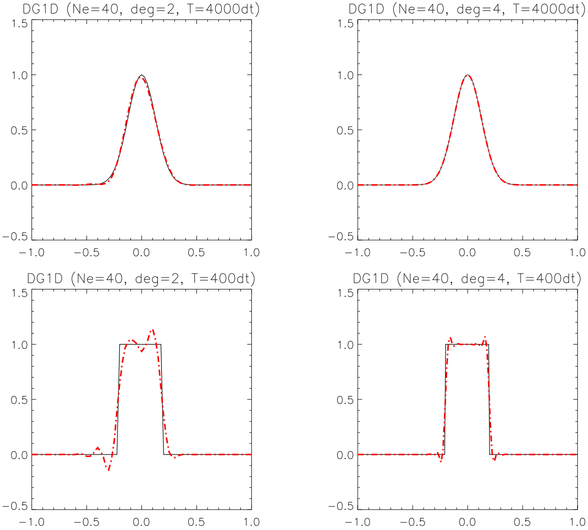

Discontinuous Galerkin (DG) Methods in 2D Cartesian Geometry

2D Scalar conservation law:

$$\frac{\partial U}{\partial t} + \nabla \cdot \mathbf{F}(U) = S(U), \quad \text{in} \quad (0, T) \times \mathcal{D}; \quad \forall (x^1, x^2) \in \mathcal{D},$$

where $U = U(x^1, x^2, t)$, $\nabla \equiv (\partial/\partial x^1, \partial/\partial x^2)$, $\mathbf{F} = (F, G)$ is the flux function, and S is the source term.

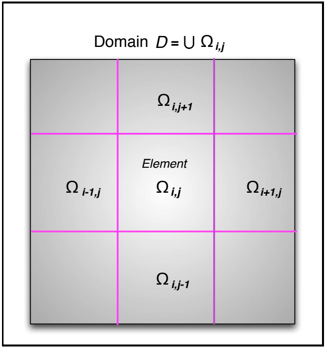

- The domain $\mathcal{D}$ is partitioned into non-overlapping elements Ω_{ij}
- Element edges are discontinuous
- Problem is locally solved on each element Ω_{ij}

DG-2D Spatial Discretization for an Element Ω_e in $\mathcal{D}$

- Approximate solution U_h belongs to a vector space $\mathcal{V}_h$ of polynomials $\mathcal{P}_N(\Omega_e)$.
- The Galerkin formulation: Multiplication of the basic equation by a *test function* $\varphi_h \in \mathcal{V}_h$ and integration over an element Ω_e with boundary Γ_e,

$$\int_{\Omega_e} \left[\frac{\partial U_h}{\partial t} + \nabla \cdot \mathbf{F}(U_h) - S(U_h) \right] \varphi_h d\Omega = 0$$

- Weak Galerkin formulation : Integration by parts (Green's theorem) yields:

$$\frac{\partial}{\partial t} \int_{\Omega_e} U_h \, \varphi_h \, d\Omega - \int_{\Omega_e} \mathbf{F}(U_h) \cdot \nabla \varphi_h \, d\Omega \quad + \int_{\Gamma_e} \mathbf{F}(U_h) \cdot \vec{n} \, \varphi_h \, d\Gamma = \int_{\Omega_e} S(U_h) \, \varphi_h d\Omega$$

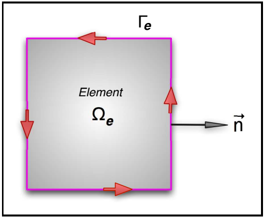

- Orthogonal polynomials (basis functions) are employed for approximating U_h and φ_h on Ω_e.
- Surface and line integrals are evaluated with high-order Gaussian quadrature rule
- Exact Integration: The flux (line) integral should be an order higher than the surface integral *(Cockburn & Shu, 1989)*.

DG-2D: High-Order Nodal Spatial Discretization

- The nodal basis set is constructed using a tensor-product of Lagrange polynomials $h_i(\xi)$, with roots at Gauss-Lobatto-Legendre (GLL) or Gauss-Legendre (GL) quadrature points $\{\xi_i\}$.

$$[h_i(\xi)]_{GLL} = \frac{(\xi^2 - 1)\, P_N'(\xi)}{N(N+1)\, P_N(\xi_i)\, (\xi - \xi_i)}; \qquad \int_{-1}^{1} h_i(\xi) h_j(\xi) \simeq w_i \delta_{ij}.$$

- $P_N(\xi)$ is the N^{th} degree Legendre polynomial; and w_i are Gauss quadrature weights

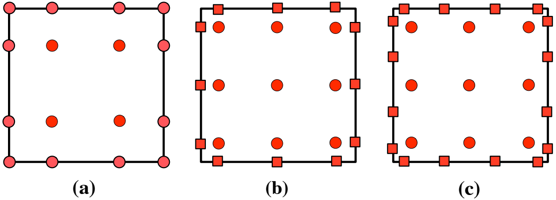

The approximate solution U_h and test function are represented in terms of nodal basis set.

$$U_{ij}(\xi, \eta) = \sum_{i=0}^{N} \sum_{j=0}^{N} U_{ij}\, h_i(\xi)\, h_j(\eta) \quad \text{for} \quad -1 \le \xi, \eta \le 1,$$

The DG, SE & FV Methods

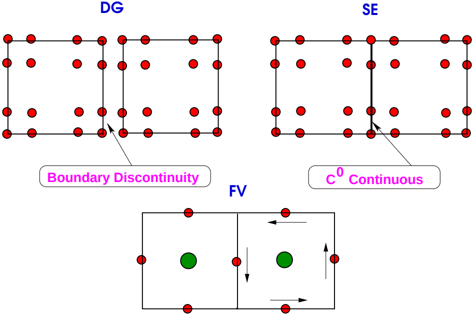

- For DGM degrees of freedom *(d.o.f)* to evolve per element is N^2, where N is the order of accuracy.
- For FV method the *d.o.f* is 1 (cell-average), irrespective of order of accuracy.
- DGM is based on conservation laws but exploits the spectral expansion of SE method and treats the element boundaries using FV "tricks."

Monotonic Limiter for DG transport

- Importance:
  - In atmospheric models, mixing ratios of the advecting chemical species and humidity should be non-negative and free from spurious oscillation.
  - The model should avoid creating unphysical negative mass
- Challenges:
  - Godunov theorem (1959): "Monotone scheme can be at most first-order accurate"
  - There is a "conflict of interest" between the high-order methods and monotonicity preservation!
  - In principle, a limiter should eliminate spurious oscillation and preserve high-order nature of the solution to a maximum possible extent
- Existing Limiters for DGM:
  - Minmod limiter (Cockburm & Shu, 1989): Based on van Leer's slope limiting, but too diffusive
  - Limiters based on WENO or H-WENO (Qui & Shu 2005), Expensive and no positivity preservation
  - New bound-preserving limiter: Positivity-preserving and local (Zhang & Shu, 2010)

Local Bound-Preserving Limiter for DGM

- If the global maximum M and minimum m values of the solution $\rho_{i,j}(x,y)$ is known, then the limited solution $\tilde{\rho}_{i,j}(x,y)$:

$$\tilde{\rho}_{i,j}(x,y) = \hat{\theta}\,\rho_{i,j}(x,y) + (1-\hat{\theta})\,\bar{u}_{i,j}, \quad \hat{\theta} = \min\{|\frac{M-\bar{u}_{i,j}}{M_{i,j}-\bar{u}_{i,j}}|, |\frac{m^*-\bar{u}_{i,j}}{m^*_{i,j}-\bar{u}_{i,j}}|, 1\},$$

- $\bar{u}_{i,j}$ is the average solution in the element $\Omega_{i,j}$, $M_{i,j} = \max_{(x,y)\in\Omega_{i,j}} \rho_{i,j}(x,y)$ and $m^*_{i,j} = \min_{(x,y)\in\Omega_{i,j}} \rho_{i,j}(x,y)$.
- $\hat{\theta} \in [0,1]$. The positivity preserving option is a special case of BP filter, and can be achieved my setting $m^* = 0$.
- This limiter is conservative and local to the element (Zhang & Shu, JCP, 2010)

DG Advection on 2D Cartesian Grid (Solid-Body Rotation)

- A DG P^2 (third-order) Model version with 6 DOFs on 3×3 G-L grid (*Zhang & Nair, MWR, 2012*)
- Solid-body rotation (Leveque, 2002) , 80×80 elements.

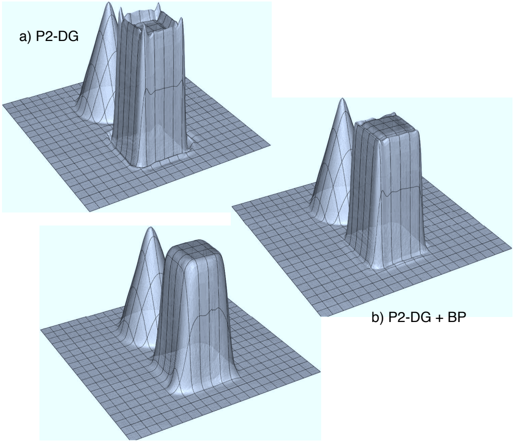

c) P2-DG + H-WENO + BP

DG Advection on 2D Cartesian Grid

- HWENO uses 3×3 cells and completely removes oscillation, but more diffusive.

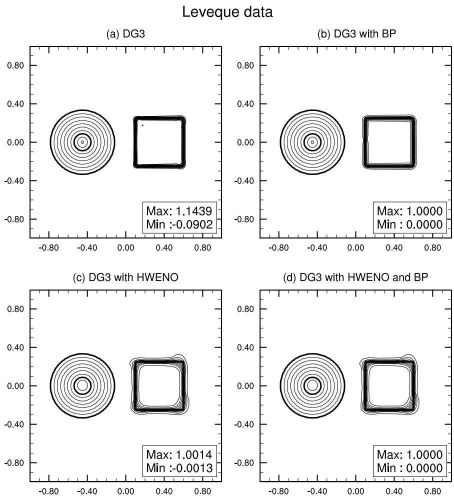

DG-2D: Scaling Results (Levy, Nair & Tufo, 2007)

- Problem: Advection of a Gaussin-hill, 80×80 elements with 6×6 GLL grid
- Strong scaling is measured by increase the number processes running while keeping the problem size constant
- Weak scaling is measured by scaling the problem along with the number of processors, so that work per process is constant

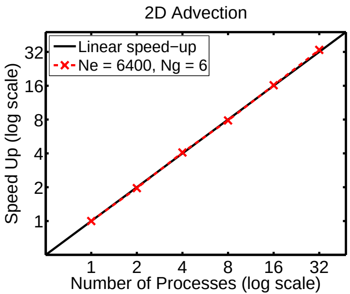

Strong scaling

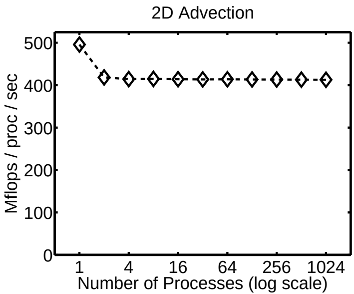

Weak scaling

Extending DG Methods to Spherical Geometry: Various Grid Options

- DG method can be potentially used on various spherical mesh with triangular or quadrilateral (or both) elements

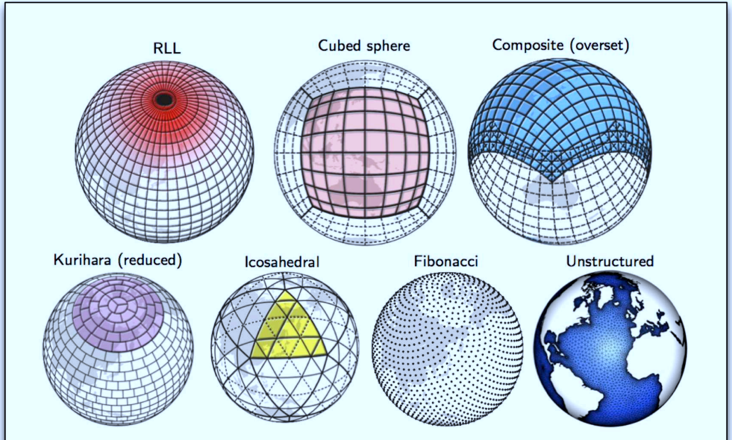

Figs source David Hall

Cubed-Sphere: Central Equiangular (Gnomonic) Projection

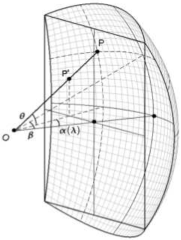

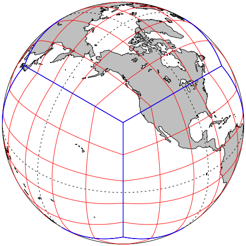

- The sphere is decomposed into 6 identical regions, and free of polar singularities (*Sadourny, MWR, 1972*).
  - Equiangular projection using central angles (x^1, x^2).
  - Non-orthogonal grid lines and discontinuous edges
  - All the grid lines are great-circle arcs
  - Quasi-uniform rectangular mesh, well suited for the element-based methods such as DG or SE methods (CAM-HOMME)

Non-Orhogonal Cubed-Sphere Grid System

Metric term (Jacobian) of [Cubed-Sphere $\rightleftharpoons$ Sphere] Transform on the cubed-sphere: $\sqrt{G}$

Central angles $(x^1, x^2) \in [-\pi/4, \pi/4]$, $(\Delta x^1 = \Delta x^2)$ are the independent variables.
Transport equation (*Nair et al. MWR, 2005*):

$$\frac{\partial}{\partial t}(\sqrt{G}\, h) + \frac{\partial}{\partial x^1}(\sqrt{G}\, u^1 h) + \frac{\partial}{\partial x^2}(\sqrt{G}\, u^2 h) = 0$$

Computational domain is the surface of cube $[-\pi/4, +\pi/4]^3$

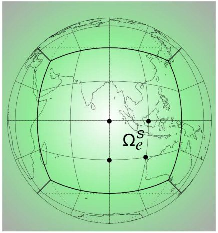

Physical Domain

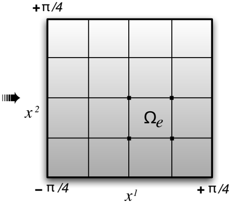

Computational Domain

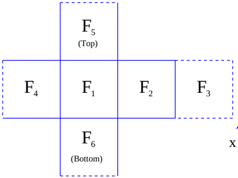

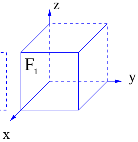

Advection: Deformational Flow (Moving Vortices on the Sphere)

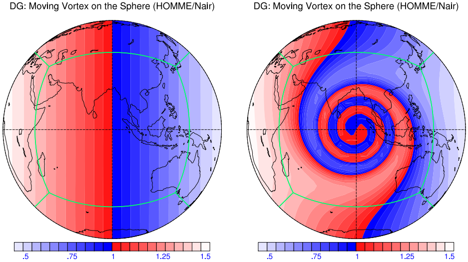

Initial field and DG solution after 12 days. Max error is $\mathcal{O}(10^{-5})$

A Smooth Deformational Flow Test *[Nair & Jablonowski (MWR, 2008)]*

- The vortices are located at diametrically opposite sides of the sphere, the vortices deform as they move along a prescribed trajectory.
- Analytical solution is known and the trajectory is chosen to be a great circle along the NE direction ($\alpha = \pi/4$).

- Deformational flow: Fine filament preservation (*Zhang & Nair, MWR, 2012*)
- Modal P^2-DG with $100 \times 100 \times 6$ cells, $\Delta t = 600$s, 60-day simulation

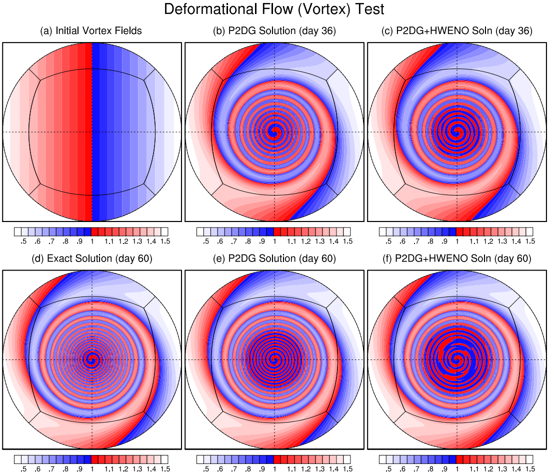

DGM Advection: Deformational flow (Slotted-Cylinder)

- Deformational flow (non-smooth deformation) (*Nair & Laurtitzen, JCP, 2010*)
- Modal P^2-DG with $45 \times 45 \times 6$ cells, $\Delta t = 0.00125$s, $T = 5$.

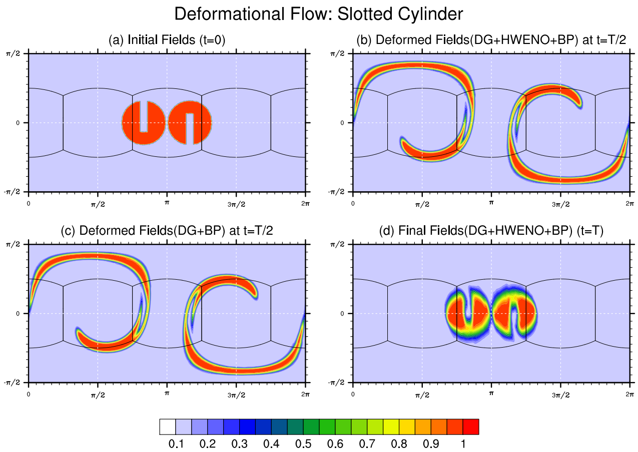

DG on Yin-Yang Overset Spherical Grid [Kageyama and Sato (2004)]

- It avoids the pole problem of the RLL grid, and there are no singular points.
- The grid spacing is quasi-uniform with a largest to smallest grid-length ratio $\sqrt{2}$
- Each grid component is orthogonal, producing a simple analytical form for PDEs.
- Overlap regions provide two set of solution.
- Numerical schemes require special treatment for conservation

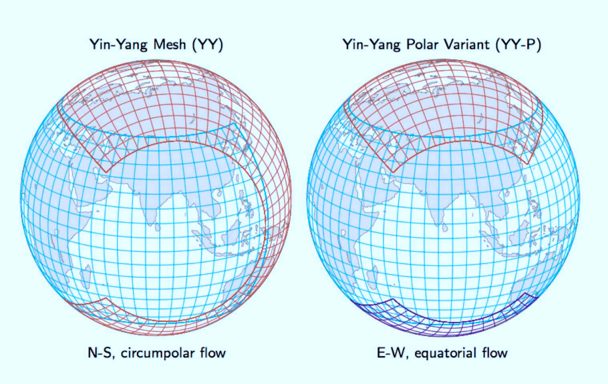

DG on Yin-Yang Grid: Advection [Hall & Nair, MWR, 2012]

- Sphere $\mathcal{S} = Y \cup Y'$ where Y: Yin region, and Y': Yang region. $Y \perp Y'$
- Y is a rectangular region in lat/lon (θ, λ)-space, $\lambda \in [-3\pi/2 - \delta, 3\pi/2 + \delta]$, $\theta \in [-\pi/4 - \delta, \pi/4 + \delta]$ where δ is the overlap region.
- There are total $6 \times N_e^2$ elements (DOF) for the DG spatial discretization.

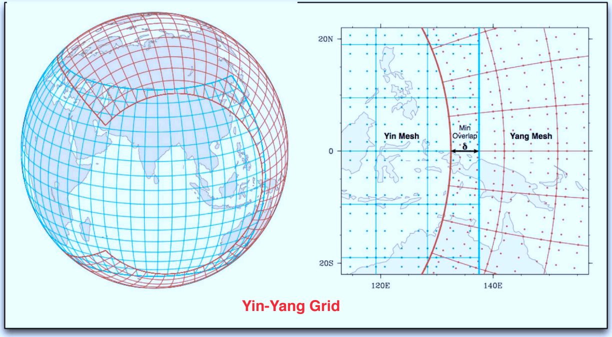

Yin-Yang Grid

DG Advection on YY Grid: Cosine-Bell Test (Time-traces of $\ell_1, \ell_2, \ell_\infty$ errors)

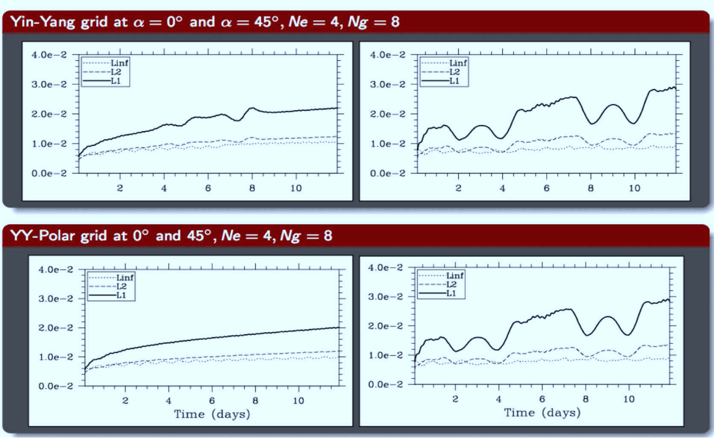

- Cosine bell transport results with $N_e = 4$ and $N_g = 8$ nodes per element (approximately 3.2° resolution, and 6144 DOF).
- Figs from *Hall & Nair, MWR, 2012*
- Note: Exact mass conservation can be enforced by additional integral constraints (*Baba et al. (2010), Peng et al. (2006)*)

DGM Convergence: Gaussian Advection and Spectral Convergence

- Advection of a Gaussian Profile (*Levy et al. 2007; Hall & Nair, MWR, 2012*)

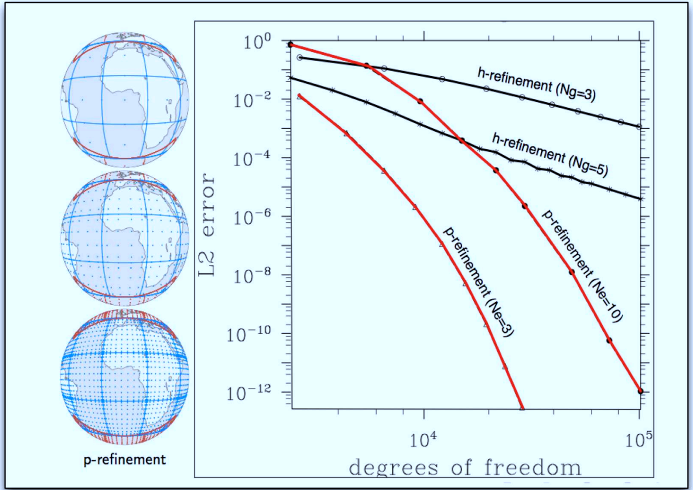

Beyond Advection: DG-3D Model Vs. CAM Spectral Models

- DG-3D Hydrostatic Dycore (*Nair et al. Comput. & Fluids, 2009*)
- JW-Baroclinic Instability Test, Day 8 Ps ($\approx 1^\circ$ resolution)
- The DG Solution is smooth and free from "spectral ringing".

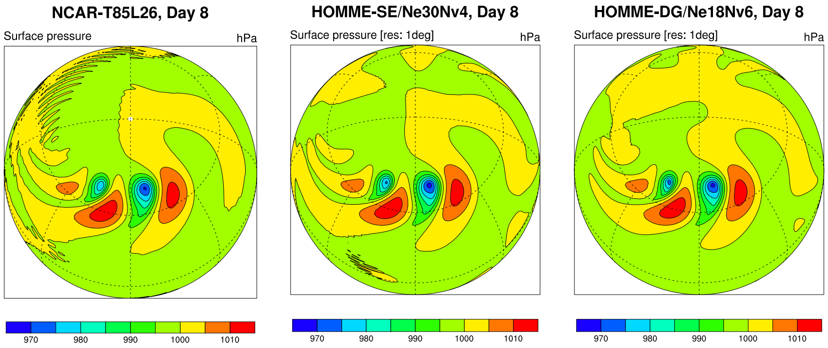

Part-II

- The quasi-Lagrangian coordinates for advection problems

Hydrostatic Equations in Flux Form: Curvilinear (x^1, x^2, η) coordinates

$$
\begin{aligned}
\frac{\partial u_1}{\partial t} + \nabla_c \cdot \mathbf{E}_1 + \dot{\eta}\frac{\partial u_1}{\partial \eta} &= \sqrt{G}u^2\,(f+\zeta) - R\,T\frac{\partial}{\partial x^1}(\ln p) \\
\frac{\partial u_2}{\partial t} + \nabla_c \cdot \mathbf{E}_2 + \dot{\eta}\frac{\partial u_2}{\partial \eta} &= -\sqrt{G}u^1\,(f+\zeta) - R\,T\frac{\partial}{\partial x^2}(\ln p) \\
\frac{\partial}{\partial t}(m) + \nabla_c \cdot \left(\mathbf{U}^i\, m\right) + \frac{\partial(m\dot{\eta})}{\partial \eta} &= 0 \\
\frac{\partial}{\partial t}(m\Theta) + \nabla_c \cdot \left(\mathbf{U}^i\,\Theta\, m\right) + \frac{\partial(m\dot{\eta}\,\Theta)}{\partial \eta} &= 0 \\
\frac{\partial}{\partial t}(mq) + \nabla_c \cdot \left(\mathbf{U}^i\, q\, m\right) + \frac{\partial(m\dot{\eta}\, q)}{\partial \eta} &= 0
\end{aligned}
$$

$$
m \equiv \sqrt{G}\,\frac{\partial p}{\partial \eta}, \nabla_c \equiv \left(\frac{\partial}{\partial x^1}, \frac{\partial}{\partial x^2}\right), \; \eta = \eta(p, p_s), G = \det(G_{ij}), \; \frac{\partial \Phi}{\partial \eta} = -\frac{R\,T}{p}\,\frac{\partial p}{\partial \eta}.
$$

Where m is the mass function, Θ is the potential temperature and q is the moisture variable. $\mathbf{U}^i = (u^1, u^2)$, $\mathbf{E}_1 = (E, 0)$, $\mathbf{E}_2 = (0, E)$; $E = \Phi + \frac{1}{2}\left(u_1 u^1 + u_2 u^2\right)$ is the energy term. Φ is the geopotential, ζ is the relative vorticity, and f is the Coriolis term.

[Ref: HOMME/DG, *Nair et al. Comput. & Fluids 2009*]

Vertical (quasi) Lagrangian Coordinates *(Starr, J. Meterol. 1945)*

A "vanishing trick" for vertical advection terms!

- Terrain-following Eulerian surfaces are treated as material surfaces ($\dot{\eta} = 0$).
- Simplified hydrostatic equations with no "vertical terms"
- The resulting Lagrangian surfaces are free to move up or down direction.

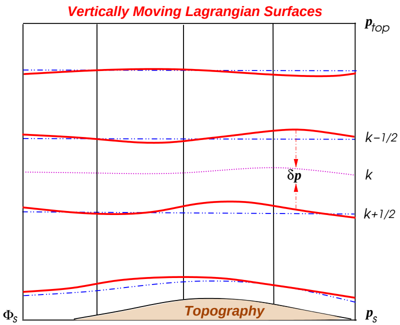

Vertically moving Lagrangian Surfaces

- Over time, Lagrangian surfaces deform and must be remapped.
- The velocity fields (u_1, u_2), and total energy (Γ_E) are remapped onto the reference coordinates.

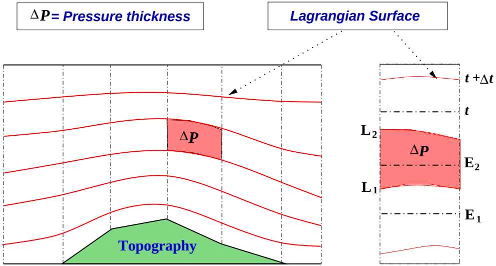

Terrain−following Lagrangian control−volume coordinates

Remapping: Lauritzen & Nair, MWR, 2008; Norman & Nair, MWR, 2008)

Remapping (Rezoning or Re-gridding) on a 1D Grid

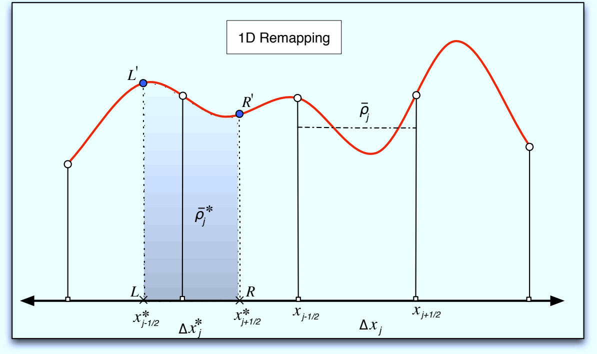

- Remapping: Interpolation from a source grid to target grid with constraints (conservation, monotonicity, positivity-preservation etc.).
- Application: Conservative semi-Lagrangian methods (e.g. CSLAM); Grid-to-grid data transfer for pre- or post-processing (GeCore).

Remapping (Rezoning or Re-gridding) on a 1D Grid

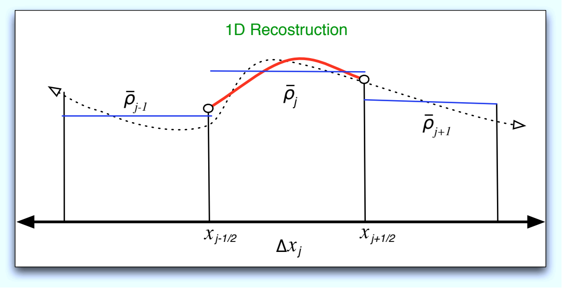

- Reconstruction: Fit a piecewise polynomial $\rho_j(x)$ for every cell $\Delta x_j = x_{j+1/2} - x_{j-1/2}$, using the known cell-average values $\bar{\rho}_j$ from the neighboring cells.
- The subgrid-scale distribution $\rho_j(x)$ must satisfy the conservation constraint:

$$\bar{\rho}_j = \frac{1}{\Delta x_j} \int_{x_{j-1/2}}^{x_{j+1/2}} \rho_j(x) dx, \quad \Rightarrow \text{Mass} = \bar{\rho}_j \, \Delta x_j$$

- $\rho_j(x)$ may be further modified to be monotonic (E.g: PLM, PPM, PCM, PHM)

Remapping 1D Grid

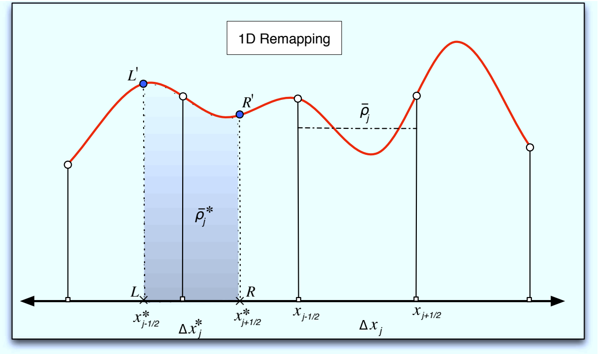

- Mass in the target cell ($\Delta x_j^* = x^*_{j+1/2} - x^*_{j-1/2}$) can be expressed as the difference of "Accumulated Mass" ($\mathcal{A}_m$):

$$\bar{\rho}_j^* \, \Delta x_j^* = \mathcal{A}_m(RR') - \mathcal{A}_m(LL') \implies \bar{\rho}_j^* = \frac{1}{\Delta x_j^*}[\mathcal{A}_m(RR') - \mathcal{A}_m(LL')]$$

where

$$\mathcal{A}_m(RR') = \int_{x_{Ref}}^{x^*_{j+1/2}} \rho(x)dx = \sum_{k=1}^{j-1} \bar{\rho}_k \, \Delta x_k + \int_{x_{j-3/2}}^{x^*_{j+1/2}} \rho_{j-1}(x)dx$$

Vertical Advection with Lagrangian η-Cooridate

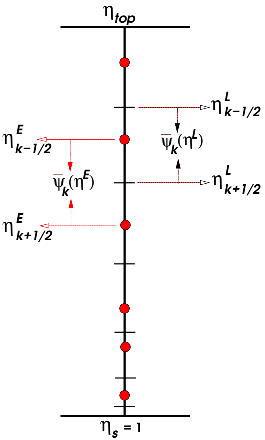

- Reference (initial) grid $\eta = \eta(P, P_s) \in [\eta_{top}, 1]$
- Source grid = Lagrangian η^L_k
- Target grid = Eulerian η^E_k; $\quad \sum \Delta\eta^E_k = \sum \Delta\eta^L_k$
- Lagrangian η^L_k can be computed from the predicted "pressure thickness" ΔP (CAM-FV)
- Remapping is performed at every advective Δt
- Every 1D vertical trajectory information can be "recycled" for all tracers

3D Transport (CAM-SE): SE horizontal + vertical remapping

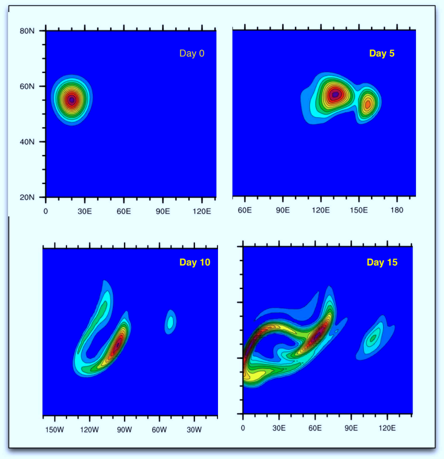

- CAM-SE (1°): JW-Test divergent flow field. SE horizontal transport is quasi-monotonic
- $\Delta t_a = 4 \times 90$ s, vertical remapping by PCM (Zerroukat, 2005) for advection.

Figure courtesy: Christoph Erath

Summary & Conclusions :

- The DG method with moderate order (third or fourth) is an excellent choice for transport problems as applied in atmospheric sciences. DGM addresses:
  1. High-order accuracy
  2. Geometric flexibility
  3. Positivity-preserving advection
  4. High parallel efficiency
  5. Local and global conservation
- In comparison with finite-volume and finite-difference implementations of the Yin-Yang grid, the DG approach is considerably simpler as the overset interpolation is local, requiring information from the interior of a single element.
- In general, modified YY-P and YY meshes exhibited similar performance on most tests, while the YY-P mesh performed better on cases with strictly zonal flow.
- DG method is an ideal candidate for the new generation petascale-capable dynamical cores.
- The "moving" vertical Lagrangian (evolve and remap approach) method provides an efficient way for 3D conservative multi-tracer transport.

THANK YOU!